Multiaxial fatigue damage estimation of structures under random vibrations using Matsubara's criterion

A. Yaich, A. El Hami

Version of Record: https://www.sciencedirect.com/science/article/pii/S0142112319300696
Manuscript_e2c04a2fbc8742398a7db9859fbf57cb

Multiaxial fatigue damage estimation of structures under random vibrations using Matsubara's criterion

A. Yaich[a] , A. El Hami[a]

[a] *Laboratory of Mechanic of Normandy, INSA Rouen, 76801 St Etienne du Rouvray, France*

Abstract:

The purpose of such a multiaxial fatigue damage criterion is to estimate the life time of structures subject to multiaxial loads. Therefore, several methods are developed to achieve this purpose. Comparing with other criteria, Matsubara's criterion predicts the fatigue damage with higher accuracy. However, this method has been applied only for constant amplitude loading. But, in real mechanical application structures are subject to random vibrations. So, in this paper we propose an extension of this criterion in the case of random structures under random vibrations, using a computationally efficient multiaxial fatigue damage strategy developed in frequency domain. Matsubara's criterion is constituted of two parameters: one governing crack initiation, and the other governing crack growth. Each parameter will be calculated from the stresses Power Spectral Densities determined at each point of the structure. A time domain formulation is also proposed in order to compare the two strategies. Two numerical applications are then used, at the end of this paper, to present the advantages of the frequency domain strategy of Matsubara's criterion for treating problem of multiaxial fatigue damage of structures under random loads.

Nomenclature:

$\sqrt{J_{2,a}}$	Equivalent shear stress amplitude	S_{max}	Matsubara's proposed Parameter
$p(t)$	Hydrostatic stress	$D_{Crossland}$	Fatigue damage using Crossland's criterion
α, β	Material parameters for criterion	D_{Sines}	Fatigue damage using Sines's criterion
$s_{i,j}$ $(i, i = x, y, z)$	Stress component	$D_{Matsubara}$	Fatigue damage using Matsubara's criterion
$\sigma_{i,j}$ $(i, i = x, y, z)$	Deviatoric stress component	E_S_{max}	Matsubara's parameter for random load
σ_W	Fully reversed axial fatigue limit	Φ_s	Stress PSD matrix
σ_T	True fracture strength	s_c	Von Mises stress
R_m	Tensile strength	Σ	covariance matrix
T	Duration of the random Gaussian load	N_p	Number of maxima
t	Time	m_i	Spectral moment
f	Frequency	σ_s	Standard deviation of *s*

1 Introduction

In real life, many structures are subjected to complex multiaxial random load. In order to determine their fatigue life, many criteria have been elaborated, mostly in time domain. In order to minimize the computing time, the fatigue damage analyses should be done in the frequency domain. This can be seen in many works such as Pitoiset X. et al [1] [2] which defined a

formulation of Matake's criterion and Crossland's criterion in frequency domain. Also, Lambert S. et al [3] [4] [5] proposed a new formulation of the Sines criterion developed in the frequency domain which took the consideration the width of the band of the excitation, and the disproportionate of random loads. Cristofori A. et al [6] proposed a frequency-domain formulation of a stress invariant based multiaxial fatigue criterion, called ''Projection by Projection'' (PbP) approach. Carpinteri A. et al [7] developed a reformulated frequency-domain critical-plane criterion in order to improve its accuracy in terms of fatigue life estimation for smooth metallic structural components under multiaxial random loading. A review of multiaxial fatigue criteria for random variable amplitude loads is presented in [8] where time and frequency domain approaches are examined. Also, a discussion of the recent developments in multi-axial spectral methods is presented in [9].

Such a multiaxial fatigue criterion leads to determine the location of the critical point in a structure. Many studies assumed, that the crack initiation is governed by the second invariant of the deviator stress tensor [10] [11]. This can be seen in the Crossland's criterion (Eq. (1)) and Sines Criterion (Eq. (2))

$$D_{Crossland} = \frac{\sqrt{J_{2,a}} + \alpha \max\limits_{0 \le t \le T}\{p(t)\}}{\beta} \le 1 \tag{1}$$

$$D_{Sines} = \frac{\sqrt{J_{2,a}} + \alpha \, \mathrm{E[p(t)]}}{\beta} \le 1 \tag{2}$$

Where $J_{2,a}$ present the second invariant of the deviator stress tensor, p(t) is hydrostatic stress and α and β are constants related to material proprieties.

According to Fossyth [12], fatigue fracture process can be divided into two stages: stage I defines the crack initiation mechanism and stage II defines the crack propagation mechanism. In Stage I, a slip band resulting from shear stress develops on a metal surface subjected to cyclic stress. Then, microscopic irregularities are generated which lead to cracks initiation. Regardless of the crack growth direction in Stage I, the crack grows perpendicularly to the maximum principal stress direction in Stage II. Matsubara et al [13] proposed a new multiaxial fatigue approach that uses a combination of two parameters that govern the two fatigue fracture stages. In [14] the accuracies of Matsubara's criterion are evaluated using fatigue limit data of notches and superficial small holes under combined bending and torsion stresses and combined axial

and torsion stresses determined experimentally. Then, an extension of the Matsubara's criterion was proposed [15] to predict the high- cycle life for multiaxial constant amplitude. The accuracy of Matsubara's criterion was verified comparing with other criteria such as McDiarmid criterion, Crossland criterion, B. Li criterion, Papadopoulos criterion, and Sumsel criterion, using different materials and different loading waveforms.

In a previous work, a numerical strategy for calculating the local multiaxial fatigue damage based on the frequency formulation of the Sines criterion developed in our laboratory, is proposed [16] in our laboratory. Then this strategy was coupled with Reliability-Based Design optimization methods in order to determine an optimal design of structures subject to random vibration that can guarantee a required structural reliability level considering fatigue damage [17].

In this paper, we have proposed an extension of Matsubara's criterion for structures under random vibrations cases. A numerical strategies of fatigue life prediction using the Matsubara's criterion developed in the frequency domain and time domain are developed. Note that the proposed strategy is for high cycle fatigue regime and linear materials. At the end of this paper, two examples of a 2D model of a sample plate and a 3D model of a PCB are respectively presented, to illustrate the application of the proposed strategies for the calculation of the fatigue damage. These examples demonstrate the advantages of the Matsubara's criterion in the frequency domain for treating complex structures under random vibrations.

2 Matsubara's criterion for cyclic stress states

(Eq (3)) presents the multiaxial fatigue damage criterion developed by Mastubara et al. [13] [14] [15] where α and β are constants related to material defined by (Eq (4)). Here, σ_W defines the fully reversed axial fatigue limit and σ_T is the true fracture strength which is defined as the fracture load divided by the actual final cross-sectional area. Matsubara assume that σ_T can be substituted by 1.84 times the tensile strength R_m ($\sigma_T = 1.84\ R_m$) [13].

$$D_{Matsubara} = \frac{\sqrt{J_{2,a}} + \alpha\ S_{max}}{\beta} \leq 1 \tag{3}$$

$$\begin{cases} \alpha = \dfrac{\sigma_W}{\sqrt{3}} \dfrac{1}{\sigma_T - \sigma_W} \\ \beta = \dfrac{\sigma_W}{\sqrt{3}} \dfrac{\sigma_T}{\sigma_T - \sigma_W} \end{cases} \tag{4}$$

Matsubara's criterion consists of two parameters that governs crack initiation $\left(\sqrt{J_{2,a}}\right)$ and initial crack growth (S_{max}). Here, $\sqrt{J_{2,a}}$ is the equivalent shear stress amplitude as determined in Li criterion and S_{max} is the parameter proposed by Matsubara. In fact, based on Nisitani and Yamasita works [18] [19] [20], the crack initiation parameter in Matsubara's criterion is dominated solely by the shear stress amplitude [13] and the crack growth behavior is considered to be controlled by the maximum of the stress intensity factor range [13], which is confirmed by Ohji et al in [21].

2.1 Calculation of the crack initiation parameter

Here, the crack initiation parameter, defined by the equivalent shear stress amplitude $\sqrt{J_{2,a}}$, follows that in Li criterion. In fact, the Li criterion equation is the same as that proposed by Crossland (Eq(1)) but with different definition of $\sqrt{J_{2,a}}$.

For a proportional loading, $\sqrt{J_{2,a}}$ can be defined by:

$$\sqrt{J_{2,a}} = \sqrt{\frac{1}{6}\begin{bmatrix}\left(s_{xx,a}-s_{yy,a}\right)^2+\left(s_{yy,a}-s_{zz,a}\right)^2+\left(s_{zz,a}-s_{xx,a}\right)^2\\ +6\left(s_{xy,a}-s_{yz,a}-s_{xz,a}\right)^2\end{bmatrix}} \tag{5}$$

Where $s_{ij,a}$ is the amplitude of the stress tensor which is defined by (Eq(6))

$$s_{ij,a} = \frac{\left(\underset{0\le t\le T}{max}\left[s_{ij}(t)\right]-\underset{0\le t\le T}{min}\left[s_{ij}(t)\right]\right)}{2}; i,j = x,y,z \tag{6}$$

The expression of equation (5) is not available for a non-proportional load. To this end, in order to determine $\sqrt{J_{2,a}}$, many approaches have been developed such as Li B. [22], Balthazar J.C. [23] and Bernasconi A. [24]. These definitions are confronted with experimental results in [25] [26] [27] [28] [29].

For non-proportional loading, Li [22] proposed to consider the smallest ellipse of the semi-axes R1 and R2 circumscribing the path of $\sqrt{J_{2,a}}$. Thus, $\sqrt{J_{2,a}}$ can be expressed as $\sqrt{J_{2,a}} = \sqrt{{R_1}^2+{R_2}^2}$. With the same principal, and to determine the equivalent shear stress amplitude, we consider that the semi-axes R1, R2, R3, R4 and R5 of the five-dimension ellipsoid circumscribed to the loading path of $\sqrt{J_{2,a}}$ and oriented in its principal directions. $\sqrt{J_{2,a}}$ can then be written as follows:

$$\sqrt{J_{2,a}} = \sqrt{R_1^2 + R_2^2 + R_3^2 + R_4^2 + R_5^2} \tag{7}$$

In Li criterion $\sqrt{J_{2,a}}$ is then defined as:

$$\sqrt{J_{2,a}} = \sqrt{D_{1,a}^2 + D_{2,a}^2 + D_{3,a}^2 + D_{4,a}^2 + D_{5,a}^2} = \|d_a\| \tag{8}$$

$\{D_{\mathrm{i}}\}_{i=1..5}$ are expressed using the stress tensor $\{s_{ij}\}_{i,j=x,y,z}$ or the deviator stress tensor $\{\sigma_{ij}\}_{i,j=x,y,z}$as follow:

$$d = \begin{cases} D_1 = \dfrac{\sqrt{3}}{2}\left(\dfrac{2}{3}s_{xx} - \dfrac{1}{3}s_{yy} - \dfrac{1}{3}s_{zz}\right) = \dfrac{\sqrt{3}}{2}\sigma_{xx} \\ D_2 = \dfrac{1}{2}(s_{yy} - s_{zz}) = \dfrac{1}{2}(\sigma_{yy} - \sigma_{zz}) \\ D_3 = s_{xy} = \sigma_{xy} \\ D_4 = s_{yz} = \sigma_{yz} \\ D_5 = s_{xz} = \sigma_{xz} \end{cases} \tag{9}$$

i.e.

$$d(t) = P.s(t) \tag{10}$$

With:

$$\begin{cases} d = [D_1, D_2, D_3, D_4, D_5]^T \\ s = \left[s_{xx}, s_{yy}, s_{zz}, s_{xy}, s_{yz}, s_{xz}\right]^T \\ P = \begin{bmatrix} \dfrac{\sqrt{3}}{3} & -\dfrac{\sqrt{3}}{6} & -\dfrac{\sqrt{3}}{6} & 0 & 0 & 0 \\ 0 & \dfrac{1}{2} & -\dfrac{1}{2} & 0 & 0 & 0 \\ 0 & 0 & 0 & 1 & 0 & 0 \\ 0 & 0 & 0 & 0 & 1 & 0 \\ 0 & 0 & 0 & 0 & 0 & 1 \end{bmatrix} \end{cases} \tag{11}$$

2.2 Calculation of the initial crack growth parameter

This parameter is proposed by Matsubara [13]. In fact, the crack in stage II grows perpendicularly to the maximum principal stress direction. Then, S_{max}, is defined as follows: Among the cyclic normal stresses on all the planes at a evaluate area, the cyclic normal stress with the maximum stress range is selected. The maximum stress during the selected cyclic normal stress is defined as S_{max}.

A schematic of an example of the critical area of the multiaxial stress field is shown in Figure 1. Let's consider the cyclic normal stresses s_{xx} and s_{yy} in the evaluate area. We expect that they are zero-mean stresses and $\left(s_{xx_{max}} > s_{yy_{max}}\right)$ (NOTE: this is just an example and not a hypothesis). The stress s_{xx} is the maximum ranging cyclic stress, and then S_{max} is the maximum value s_{xx_max}.

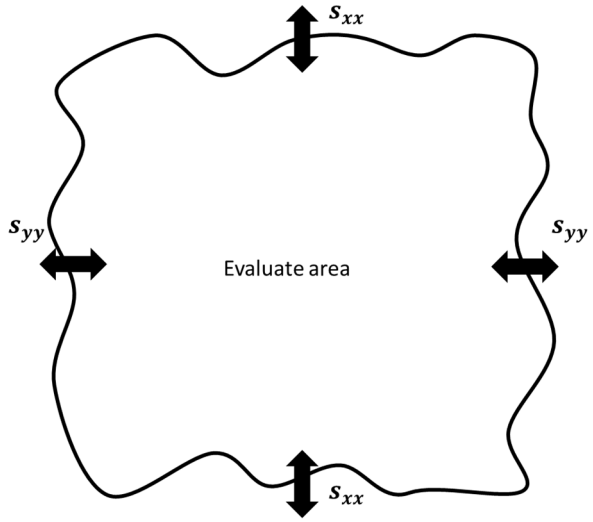

Figure 1 : Schematic of the critical area

3 Fatigue damage estimation of structures under random vibrations using Matsubara's criterion

Such a multiaxial fatigue criterion can be represented mathematically by:

$$g(s_{i,j}(t), \mathrm{T}) \leq 1 \tag{12}$$

With $s_{i,j}(t)$ is the stress tensor for any time $t \in [0, T]$ at any given location in the structure. If the inequality (12) is not satisfied, at any point of the structure, a fatigue crack can appear.

According to Pitoiset [30], the crack will initiate after a certain number of repetitions of the periodic random stationary ergodic Gaussian load of duration, *T*, if the average of the fatigue damage exceeds the fatigue limit, as presented by (Eq(13))

$$E\left[g\left(s_{i,j}(t), \mathrm{T}\right)\right] \leq 1 \tag{13}$$

Let's consider now a linear structure subject to stationary ergodic Gaussian loads. The Matsubara's criterion can then be defined by :

$$E[D_{Matsubara}] = \frac{E\left[\sqrt{J_{2,a}}\right] + \alpha\, E\_S_{max}}{\beta} \leq 1 \tag{14}$$

For a zero mean value stresses, E_S_{max} can be determined as follow: for each normal stress, we calculate the mean value of the extreme of the Gaussian process over the observation period T. the maximum of these mean values are then selected and it defines E_S_{max}. It can be mathematically presented as:

$$\mathrm{E}\_S_{max} = \max_i \left(E\left[\max_t (s_{ii}) \right] \right) \quad ; \quad i = x; y; z \tag{15}$$

For structures under random vibrations, the stresses Power Spectral Densities (PSD) are generally used in the fatigue damage analysis. Numerically, those PSDs are determined at each point of the structure using a FEM software. For a 3D model, the stress PSD matrix at a given frequency *f* can be written as:

$$\Phi_s(f) = \begin{bmatrix} \Phi_{s_{xx}s_{xx}} & \Phi_{s_{xx}s_{yy}} & \Phi_{s_{xx}s_{zz}} & \Phi_{s_{xx}s_{xy}} & \Phi_{s_{xx}s_{yz}} & \Phi_{s_{xx}s_{xz}} \\ \Phi_{s_{yy}s_{xx}} & \Phi_{s_{yy}s_{yy}} & \Phi_{s_{yy}s_{zz}} & \Phi_{s_{yy}s_{xy}} & \Phi_{s_{yy}s_{yz}} & \Phi_{s_{yy}s_{xz}} \\ \Phi_{s_{zz}s_{xx}} & \Phi_{s_{zz}s_{yy}} & \Phi_{s_{zz}s_{zz}} & \Phi_{s_{zz}s_{xy}} & \Phi_{s_{zz}s_{yz}} & \Phi_{s_{zz}s_{xz}} \\ \Phi_{s_{xy}s_{xx}} & \Phi_{s_{xy}s_{yy}} & \Phi_{s_{xy}s_{zz}} & \Phi_{s_{xy}s_{xy}} & \Phi_{s_{xy}s_{yz}} & \Phi_{s_{xy}s_{xz}} \\ \Phi_{s_{yz}s_{xx}} & \Phi_{s_{yz}s_{yy}} & \Phi_{s_{yz}s_{zz}} & \Phi_{s_{yz}s_{xy}} & \Phi_{s_{yz}s_{yz}} & \Phi_{s_{yz}s_{xz}} \\ \Phi_{s_{xz}s_{xx}} & \Phi_{s_{xz}s_{yy}} & \Phi_{s_{xz}s_{zz}} & \Phi_{s_{xz}s_{xy}} & \Phi_{s_{xz}s_{yz}} & \Phi_{s_{xz}s_{xz}} \end{bmatrix} \tag{16}$$

In the following sections, we present the fatigue damage strategies of structures under random vibrations using Matsubara's criterion developed in the time domain and frequency domain.

3.1 Time domain method

The implementation of the fatigue damage analysis strategy using Matsubara's criterion developed in the time domain is illustrated in figure 2. The algorithm consists of two subproblems: the first one, consists of the calculation of the Power Spectral Densities of the stresses. Those PSDs are determined using the finite elements software Ansys. First, we build the model by defining geometry, material proprieties and boundaries conditions. A modal analysis is then generated to determine normal modes in the excitation bandwidth. Then, a spectral analysis is needed to determine PSDs at each point of the structure. Here, excitation's PSD can be introduced as a base excitation or a nodal excitation.

In order to evaluate the fatigue damage, for the second subproblem, the calculated PSDs are then introduced into MATLAB software to generate a scalar process of the stress tensor $s_{i,j}(t)$ using the inverse FFT algorithm. This method is descripted by X. Pitoiset in [30]. Then, for each

generated time history stress tensor, the equivalent shear stress amplitude $\sqrt{J_{2,a}}$ is determined, which is given for zero-mean stresses by (Eq(17)) where $s_c(t)$ is the Von Mises stress [1] [2].

$$\sqrt{J_{2,a}} = \frac{1}{\sqrt{3}} \underset{t}{max} |s_c(t)| \tag{17}$$

For 2D stress state, s_c is defined by:

$$s_c^2 = s_{xx}^2 + s_{yy}^2 - s_{xx}s_{yy} + 3s_{xy}^2 \tag{18}$$

Also, the normal stresses maxima are determined, for each generated sample. After calculating E_S_{max} , and $E\left[\sqrt{J_{2,a}}\right]$ using equations (14-15), the estimation of the fatigue damage is finally determined.

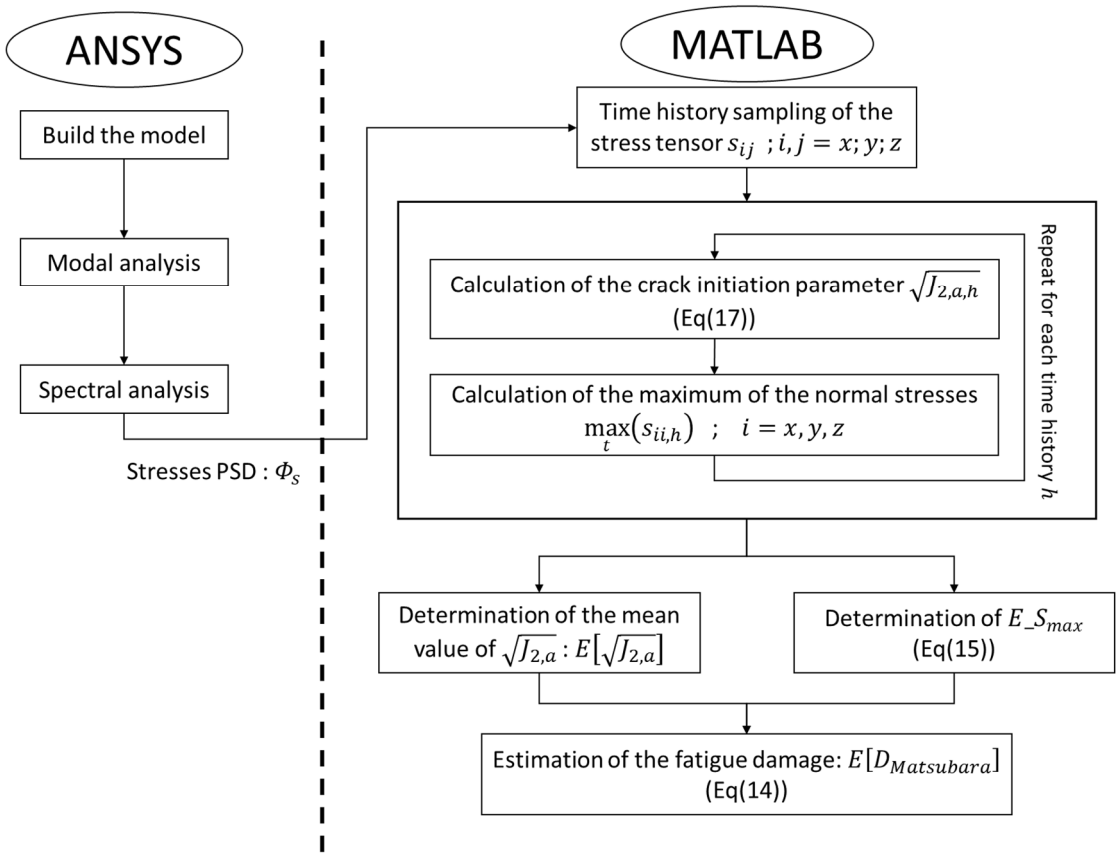

Figure 2 : Time domain method

3.2 Frequency domain method

Here, the methodology of calculation of the mean value of the first parameter of Matsubara's criterion $\sqrt{J_{2,a}}$, in the frequency domain is same as used in Sines criterion presented in previous

work [16] [17]. As defined by (Eq(7)), the estimation of the semi-axes R_i leads to estimate $\sqrt{J_{2,a}}$. The algorithm of determining of $E\left[\sqrt{J_{2,a}}\right]$ is defined as follows:

1- Calculation of the covariance matrix Σ_d of d defined by (Eq(19)). It can be determined from the covariance matrix of the stress Σ_s as presented by (Eq(20)).

$$\Sigma_d = E\left[\left(d(\mathrm{t}) - \bar{d}\right).\left(d(\mathrm{t}) - \bar{d}\right)^T\right] \tag{19}$$

$$\Sigma_d = P\Sigma_s P^T \tag{20}$$

2- The diagonal terms of Σ_d present the variance of each component. However, the terms out of diagonal present the variance between each component. In general, these terms are different from zero. So, Σ_d is not diagonal. There is an orthonormal basis of eigenvectors A_d such that:

$$\Sigma_{\tilde{d}} = A_d \Sigma_d {A_d}^T = diag(\sigma_1^2, \sigma_2^2, \sigma_3^2, \sigma_4^2, \sigma_5^2) \tag{21}$$

$with\ \sigma_1 \geq \sigma_2 \geq \sigma_3 \geq \sigma_4 \geq \sigma_5$

Then we can define a vector $\tilde{d}$ linearly associated with d by an orthogonal transformation such that:

$$\tilde{d}(\mathrm{t}) = A_d d(t) \tag{22}$$

With $\tilde{d}(\mathrm{t}) = [\widetilde{D_1}(t)\ \widetilde{D_2}(t)\ \widetilde{D_3}(t)\ \widetilde{D_4}(t)\ \widetilde{D_5}(t)]^T$

3- Calculation of the number of maxima $N_{\mathrm{p}}\left(\widetilde{D_\iota}\right)$ of each parameters of the vector $\tilde{d}$. It can be determined from the spectral moment m_i of the random process $\widetilde{D_\iota}$:

$$N_p = \sqrt{\frac{m_4}{m_2}} \tag{23}$$

$$m_i = \int_{-\infty}^{+\infty} |f|^i \Phi_{\widetilde{D_i}}(f) df \tag{24}$$

4- $E[R_i]$ can then be estimated using (Eq(25)), with $\sigma_{\widetilde{D_\iota}}$ presents the standard deviation of the random process $\widetilde{D_\iota}$ [31]

$$E[R_i] \approx \sigma_{\widetilde{D_\iota}} \left(\sqrt{2lnN_{\mathrm{p}}\left(\widetilde{D_\iota}(t)\right)} + \frac{0{,}5772}{\sqrt{2lnN_{\mathrm{p}}\left(\widetilde{D_\iota}(t)\right)}} \right), i = 1 \ldots 5 \tag{25}$$

5- For structures under random loads, $E\left[\sqrt{J_{2,a}}\right]$ can be determined by [2] [32]:

$$E\left[\sqrt{J_{2,a}}\right] \approx \sqrt{E[R_1]^2 + E[R_2]^2 + E[R_3]^2 + E[R_4]^2 + E[R_5]^2} \quad (26)$$

The problem now is determining E_S_{max}. In fact, since *s(t)* is a zero mean stationary Gaussian, random process, E_S_{max} can be obtained as follow: for each normal stress, the maximum value is estimated by applying the peak factor theory using (Eq(27)) [31] [33]. Then, E_S_{max} is obtained by applying (Eq(15)).

$$E\left[\max_t(s_{ii})\right] \approx \sigma_{s_{ii}}\left(\sqrt{2lnN_p(s_{ii}(t))} + \frac{0{,}5772}{\sqrt{2lnN_p(s_{ii}(t))}}\right) \; ; \quad i = x, y, z \quad (27)$$

Figure 3 presents the strategy implementation of the fatigue damage analysis using Matsubara's criterion developed in the frequency domain. After the determination of the matrix of stresses PSD at each point of the structure using a finite element software Ansys, we calculate $E\left[\sqrt{J_{2,a}}\right]$ and E_S_{max} as descripted before. Finally, this allow us to determine the fatigue damage at each point using Matsubara's criterion as presented by (Eq(14)).

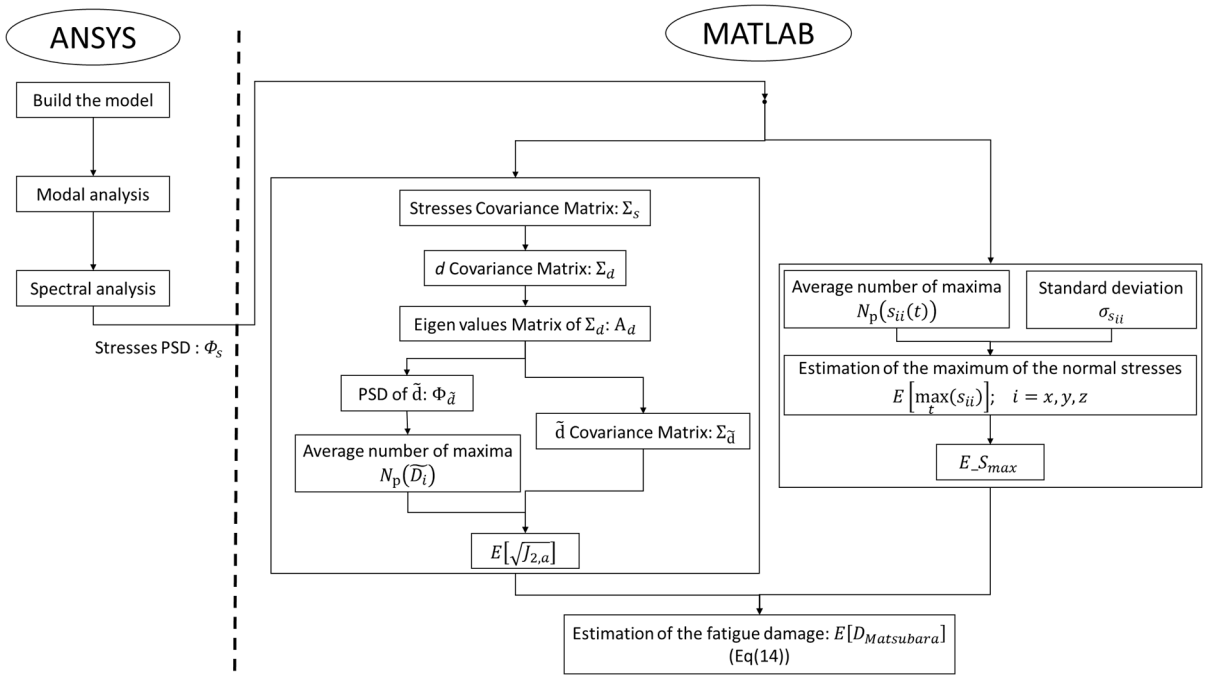

Figure 3 : Frequency domain method

4 Numerical results

4.1 2D example of sample plate

To illustrate the proposed methodology in presence of random loading, we consider an example of a 2D steel simple plate illustrated in figure 4. The sample has a hole and a notch. Its

thickness is $e = 1mm$ and clamped at both ends. Each clamp is subjected to a band-limited white noise acceleration along the normal direction to the plate plane (z) ($\Phi_a = 1g^2/Hz$; $f_c = 500Hz$) , as shown in Figure 5. Figure 5 also presents the finite element model. It was discretized into a total number of 331 shell elements. Each element has four nodes with six degrees of freedom at each node (Ansys command: SHELL181). The choice of this configuration is based on a mesh convergency study as presented in figure 6. This figure presents the evolution of the normal modes in the excitation bandwidth when changing element's number. It can be concluded that the result converges with a total number of 331 elements.

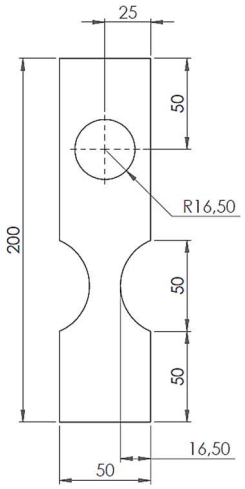

Figure 4 : Geometry of the 2D sample plate

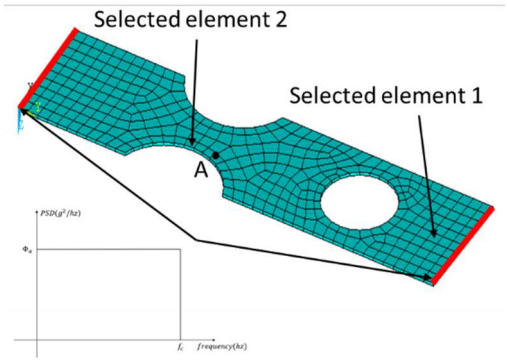

Figure 5 : Mesh and boundaries conditions

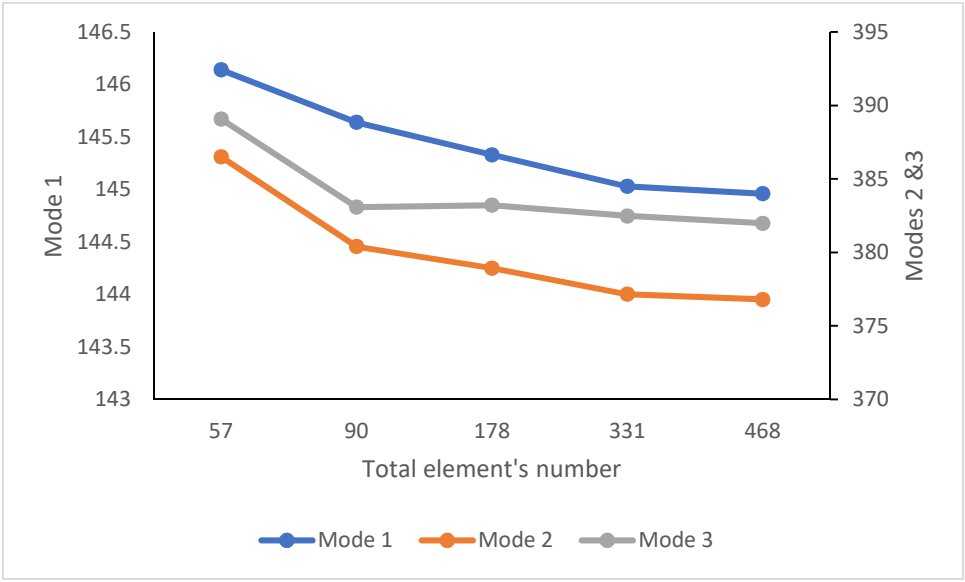

Figure 6 : Mesh convergency study

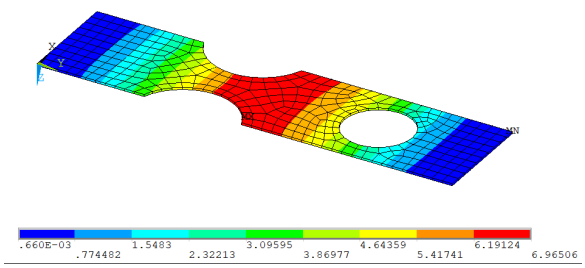

Figure 7 : Mode 1 (145.03Hz)

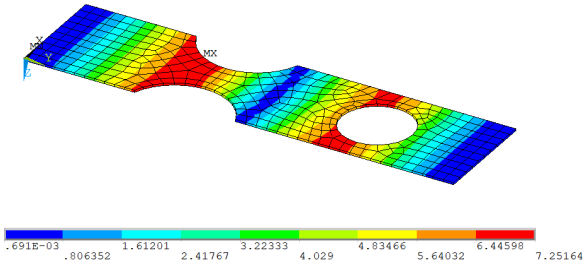

Figure 8 : Mode 2 (377.15 Hz)

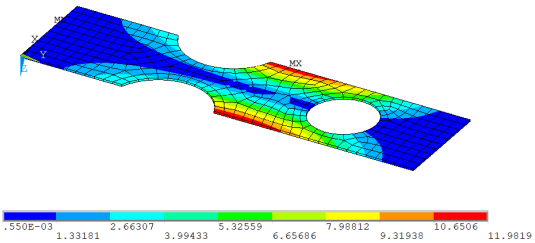

Figure 9 : Mode 3 (382.49 Hz)

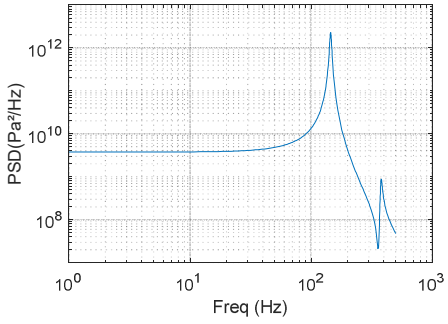

(a)

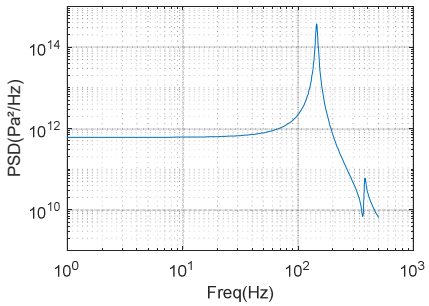

(b)

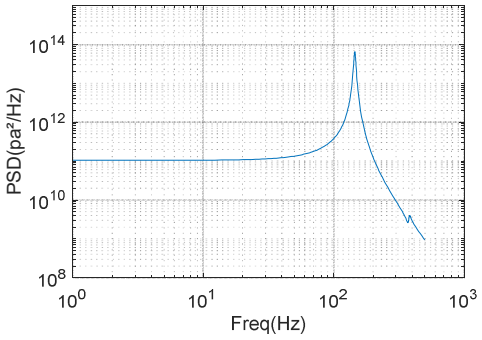

(c)

Figure 10 : Stresses PSDs (a) (a) $\Phi_{s_{xx}s_{xx}}$(b) $\Phi_{s_{yy}s_{yy}}$ (c) $\Phi_{s_{xy}s_{xy}}$

Figures 7, 8 and 9 present the first three modes within the bandwidth of the excitation. Note that the contour plots refer to plate surfaces. The material is characterized in fatigue by its fully reversed axial fatigue limit $\sigma_W = 252MPa$ and the tensile strength $R_m = 340MPa$. The PSD matrix of the stress components (Eq(16)) is calculated in every point using a random vibration code. Figure 10 presents the stresses PSDs $\Phi_{s_{xx}s_{xx}}$, $\Phi_{s_{yy}s_{yy}}$ and $\Phi_{s_{xy}s_{xy}}$ in point A (see figure 5). 1σ result of the equivalent Von Mises is presented in figure 11. This means that Von Mises stress level is at or below 1σ (68.2%), of the excitation time. It can be seen that there is a concentration of the constrain near the upper side of the notch and near the clamped sides of the plate.

In order to check the consistency of the proposed formulation, both frequency domain strategy, and time domain strategy have been applied to the sample plate. In the time domain, 100 time-histories have been generated (Monte-Carlo simulation). The results have been then averaged on these generated time-histories.

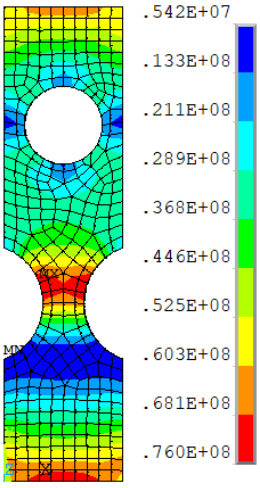

Figure 11 : 1σ *of the equivalent Von Mises result (Pa)*

Figures 12(a) and 12(b) present the fatigue map of Matsubara's criterion obtained from both frequency domain and time domain strategies. The maximum obtained value of the fatigue damage of all points are 0.977 and 0.994 respectively for frequency domain, and time domain formulations. Also, the maximum value is obtained at the same element location. The average difference of all elements between the two strategies is equal to 0.07 and the maximum difference over all elements is about 0.2.

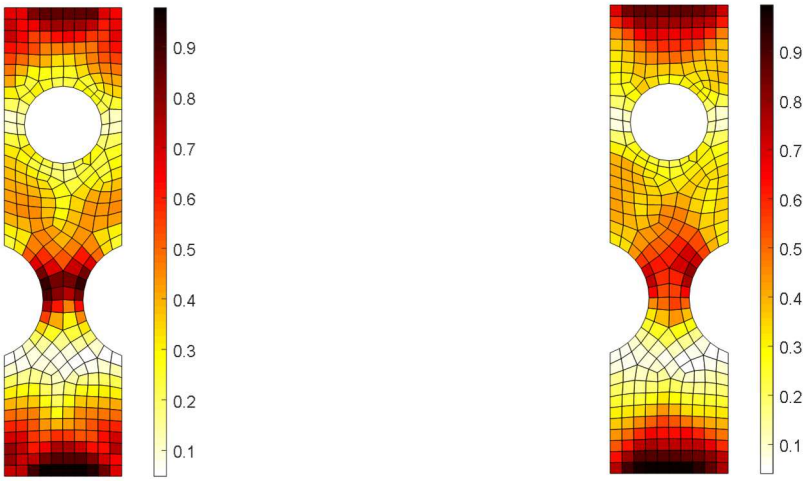

(a) (b)

Figure 12 : Fatigue damage map using Matsubara's criterion (a) frequency domain strategy (b) time domain strategy

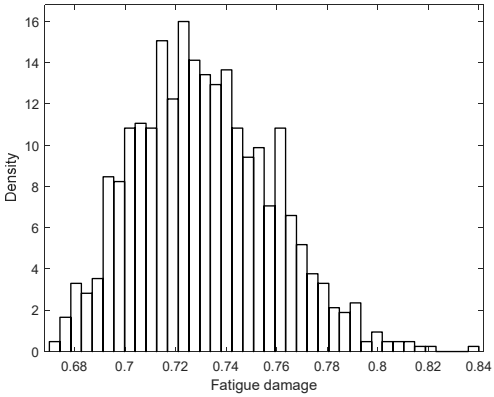

Figure 13 : PDF of fatigue damage at selected element #1

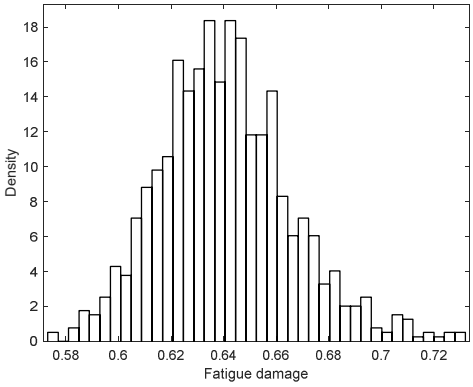

Figure 14: PDF of fatigue damage at selected element #2

The frequency domain formulation has efficiently reduced the computing time as compared to time domain formulation. In fact, the generation of the map takes about 7 s in the frequency domain against 2770s in the time domain, using PC HP with the processor Intel®Core™2.4GHz, 8 GB RAM.

The time domain algorithm allows to determine the Probability Density Function (PDF) of the fatigue damage at each point of the structure. For example, figures 13 and 14 present the Probability Density Functions (PDF) of the fatigue damage obtained at two selected elements (see figure 5), obtained using the time domain algorithm.

4.2 Application on PCB

Now, let's consider a simplified Printed Circuit Board (PCB) model on which three electronic components are placed (figure 15). Figure 16 presents its geometry. The height of each component and the PCB are descripted in table 1 where, C1, C2, and C3 are the electronic

components of the model (see figure 15). The materials proprieties of all components used in the model are presented in table 2. The PCB is meshed using 3D 20-node tetrahedral elements (Ansys command: SOLID186). A total number of 4958 elements is then obtained. A mesh convergency study is used to justify this choice. Figure 17 presents the evolution of the first five modes of the PCB when changing the mesh. It can be clearly seen that the model converges with a total number of 4958 elements. The PCB is clamped at two sides and each clamp is exposed to a white noise base acceleration PSD ($\Phi_a = 0.5g^2/Hz\,;\, f_c = 2000Hz$) as presented by figure 18.

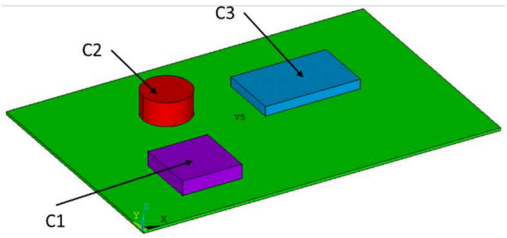

Figure 15 : 3D model of PCB

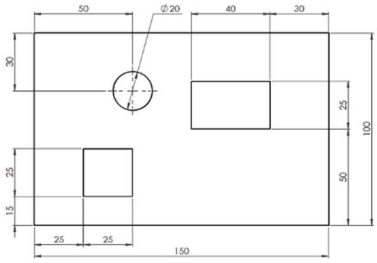

Figure 16 : PCB geometry

Table 1: : Height of components

Component	PCB	C1	C2	C3
Height (mm)	1.2	6	10	4

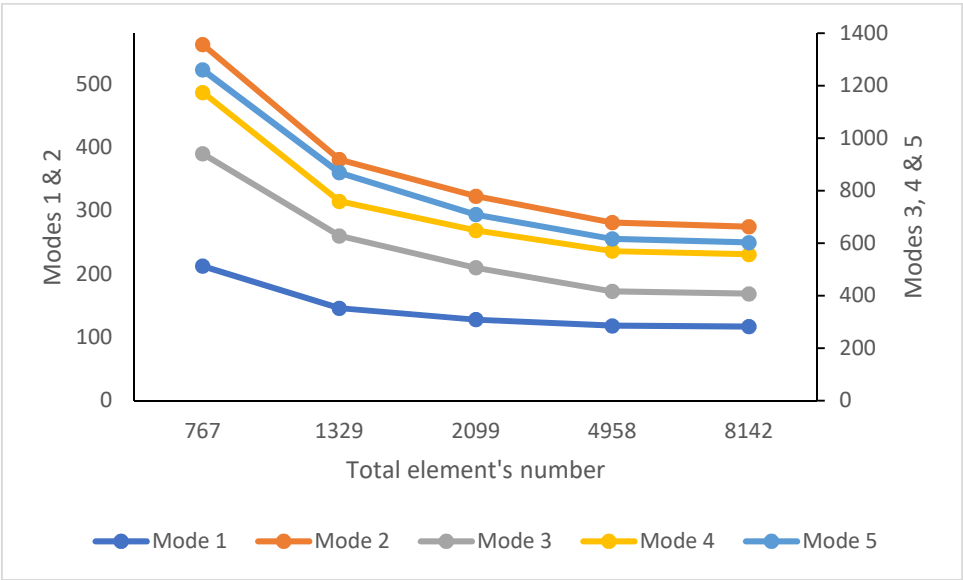

Figure 17 : Mesh convergency study

Table 2: Materials proprieties

Component	Density (kg/m^3)	Young modulus (GPa)	Poisson ration
PCB	1960	20	0.13
C1	2340	113	0.42
C2	2947	1	0.3
C3	7850	200	0.3

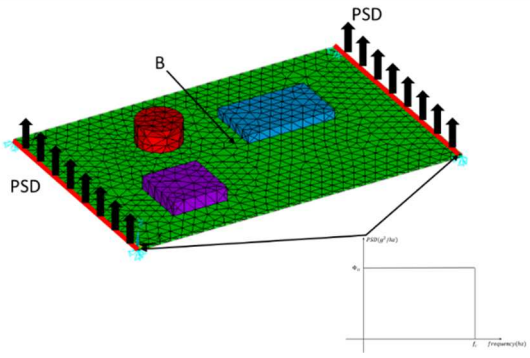

Figure 18 : Mesh and boundaries conditions

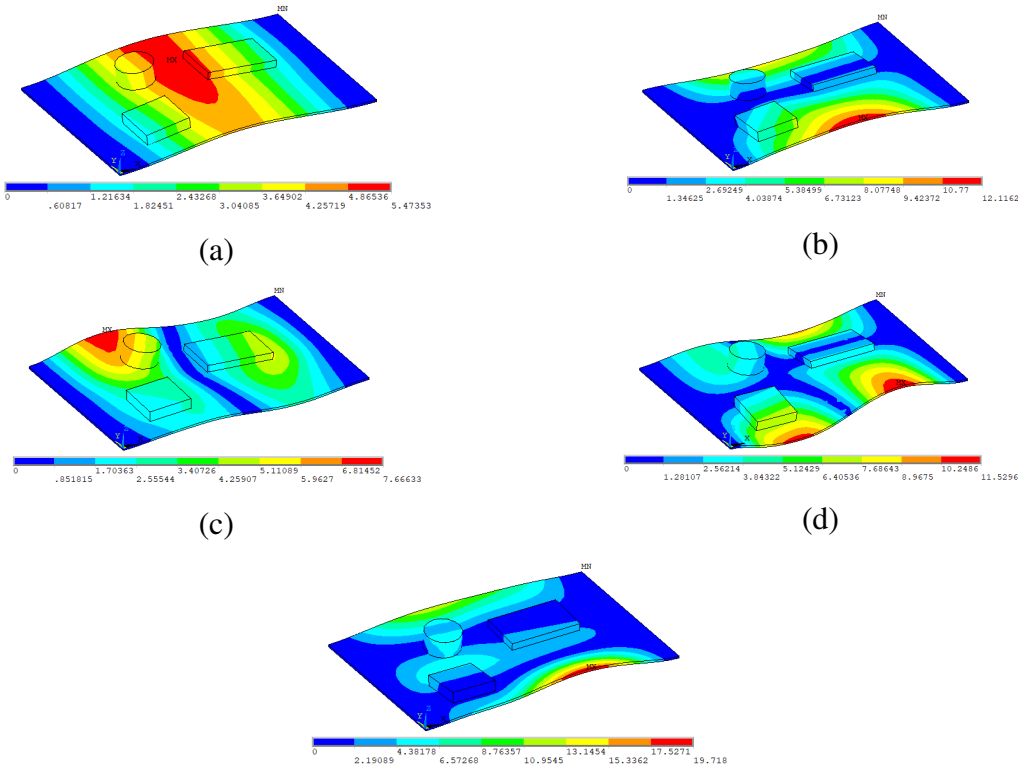

Figure 19: Modes (a) 118.09 Hz (b) 281.13 Hz (c) 416.48 Hz (d) 570.07 Hz (e) 616.75 Hz

The modal analysis leads to determine the 14 normal modes of the PCB within the bandwidth of the excitation. Figures 19 presents the first five modes. The PCB is characterized in fatigue by its fully reversed axial fatigue limit $\sigma_W = 150MPa$ and the tensile strength $R_m = 380MPa$ [34]. The spectral analysis leads to determine the stresses PSD matrix at each element of the PCB. Figure 20 presents the stresses PSDs $\Phi_{s_{xx}s_{xx}}$, $\Phi_{s_{yy}s_{yy}}$ and $\Phi_{s_{xy}s_{xy}}$ in point B (see figure 18). Those PSDs are then introduced to MATLAB in order to determine the fatigue damage using the developed strategies in time, and frequency domains. In the time domain, the fatigue damage has been meaned using 100 generated time-histories stresses (Monte-Carlo simulation).

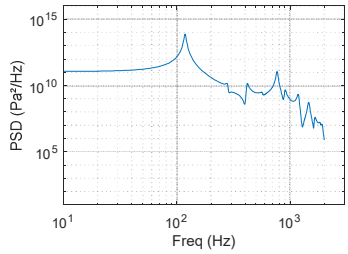

(a)

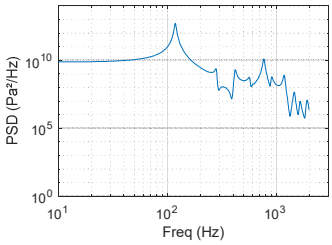

(b)

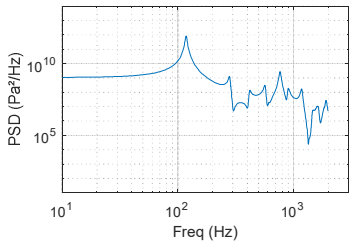

(c)

Figure 20 : Stresses PSDs (a) (a) $\Phi_{s_{xx}s_{xx}}$(b) $\Phi_{s_{yy}s_{yy}}$ (c) $\Phi_{s_{xy}s_{xy}}$

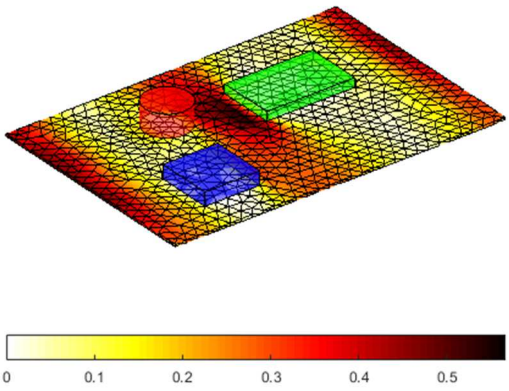

(a)

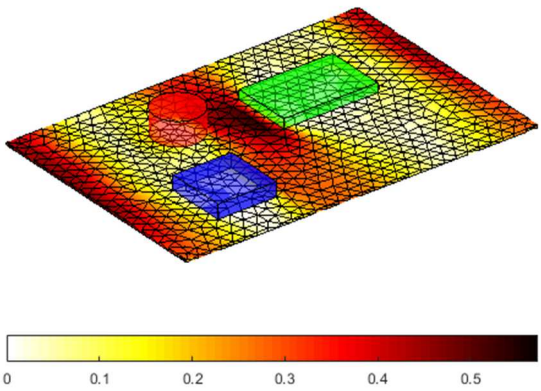

(b)

Figure 21 Fatigue damage map using Matsubara's criterion (a) frequency domain strategy (b) time domain strategy

The map of the local value of Matsubara's criterion obtained from both frequency domain and time domain strategies are presented in figures 21(a) and 21(b) respectively. It can clearly be seen that a high fatigue damage is located near to C3 component and near to the clamped sides. The maximum obtained value of the fatigue damage of all the points are 0.566, and 0.572 respectively for frequency, and time domains with a difference of 0.006, and it is located at the same point of the PCB. An average difference of 0.005 between the two formulations had been observed, and the maximum difference over all points reached 0.008.

Same as the 2D example studied previously, the frequency domain formulation has efficiently reduced the computing time comparing with the time domain formulation. The computing time to obtain the fatigue map in the frequency domain was about 50s and the computing time in the time domain was about 4 hours, using PC HP with the processor Intel®Core™2.4GHz, 8 GB RAM.

4.3 PCB optimization study

The objective now is to determine the best components position between four configurations chosen arbitrarily. Configuration 1 is shown in figure 15 and configurations 2, 3, and 4 are shown in figure 22.

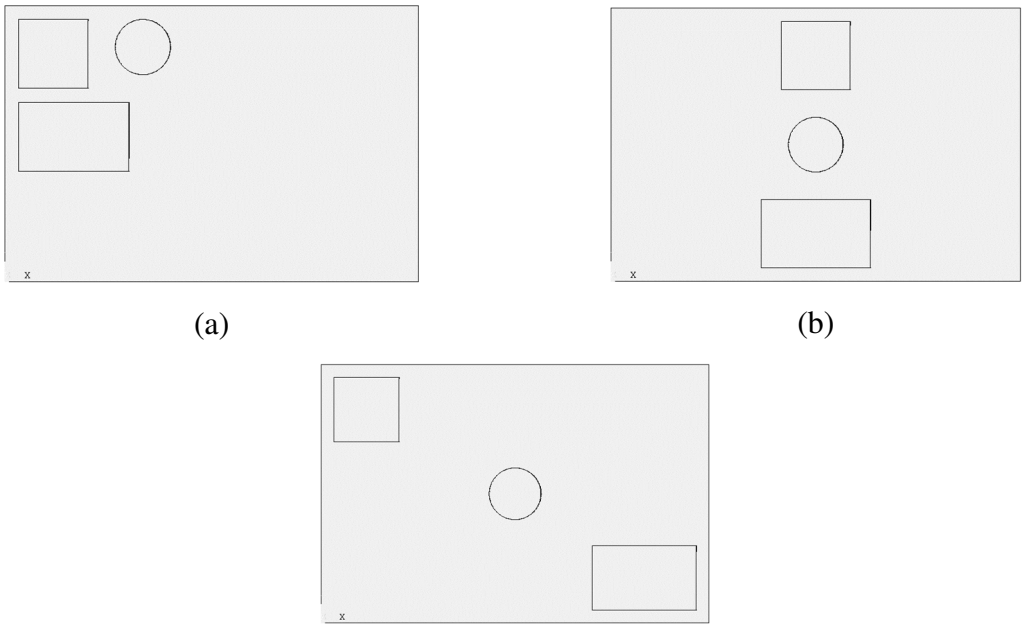

(a) (b)

(c)

Figure 22 : Studied configurations (a) configuration 2 (b) configuration 3 (c) configuration 4

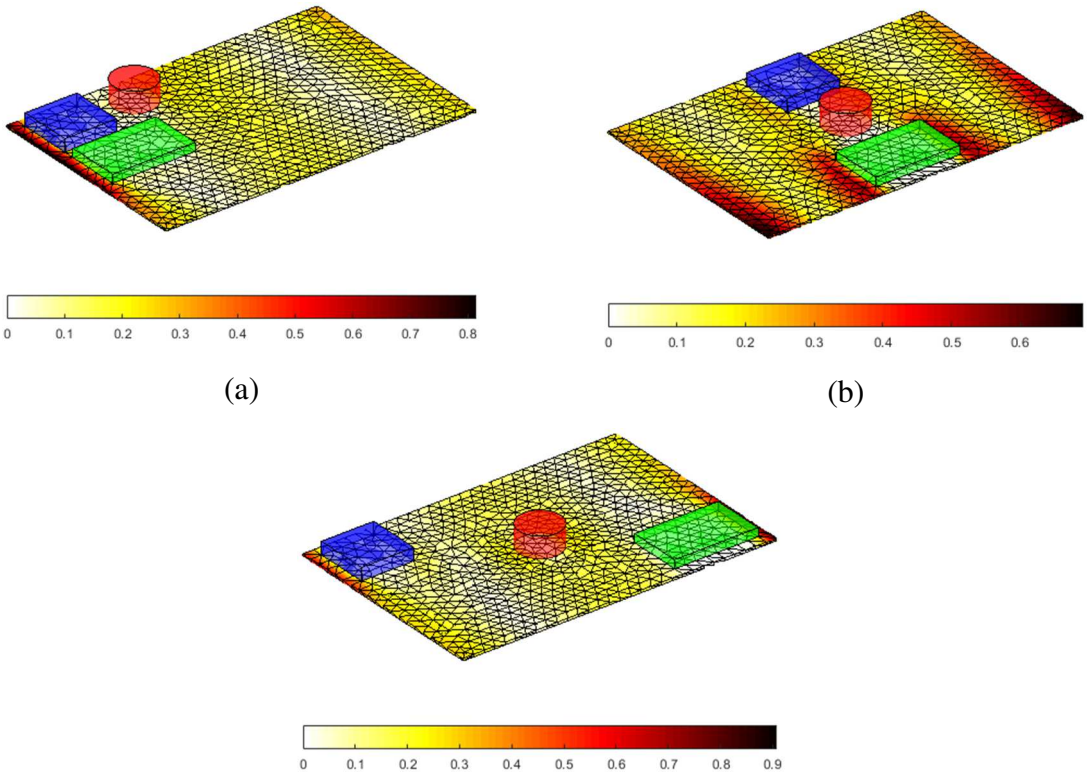

Figure 23 : Fatigue damage map (a) configuration 2 (b) configuration 3 (c) configuration 4

Figures 23 (a), (b) and (C) presents the fatigue damage map for configurations 2, 3, and 4 respectively. It interposed that the maximum fatigue damage location depends on the components' location. For configurations 1(see figure 21) and 3, the maximum fatigue damage is located near to C3 component in the middle of the PCB and near the clamped sides. But, with configurations 2 and 4, the maximum damage is located on the corners.

Table 3 describes the obtained value of the maximum fatigue damage for each configuration. Note that the first configuration presents the best components' distribution, in term of maximum fatigue damage comparing with other configurations.

Table 3 : Maximum Fatigue damage for each configuration

Configuration number	Maximum damage
1	0.566
2	0.815
3	0.692
4	0.907

5 Conclusion

The aim of this work is to develop an efficient methodology that determines the fatigue damage of structures subject to random vibrations using Matsubara's criterion. First, the formulation of Matsubara's criterion for cyclic stress state was presented. Then, two new strategies that provide maps of local fatigue damage on every points of the structure in the time domain and frequency domain are respectively proposed.

Two numerical examples, i.e. a 2D model consisting of sample plates with a hole, and a notch and a 3D model consisting of a PCB with three electronic components subject to random vibrations, demonstrate the efficiency, and the rapidity of the frequency domain formulation comparing with the time domain formulation in term of computing time. This strategy can then be coupled with the reliability-based design optimization methods to have the best design of the structure.

The different formulation descripted in this paper has been implemented in MATLAB which is used as a postprocessor of a finite element software ANSYS.

6 Acknowledgment

The present research work is a part of PISTIS Project, financed by DGA France (Postdoc position). The authors gratefully acknowledge the support of all companies in this project, specifically THALES company.

References

[1] X. Pitoiset and A. Preumont, "Spectral methods for multiaxial random fatigue analysis of metallic structures," *International Journal of Fatigue,* pp. 541-550, 2000.

[2] X. Pitoiset, I. Rychlik and A. Preumont, "Spectral methods to estimate local multiaxial fatigue failure for structures undergoing random vibrations," *Fatigue Fract Engng Mater Struct,* pp. 715-727, 2001.

[3] S. Lambert, L. Khalij, A. El Hami and E. Pagnacco, "Optimisation of structures subject to white noise random excitations considering fatigue life.," in *International Conference on Degradation, Damage, Fatigue, and Accelerated Life Models in Reliability Testing, ALT 2006*, Angers, France, 2006.

[4] S. Lambert, E. Pagnacco, L. Khalij , E. Souza de Cursi and A. El Hami, "Global optimisation of randomly excited structures with damage constraints," in *Proceedings of the XII International Symposium on Dynamic Problems of Mechanics, DINAME 2007*, Brazil , 2007.

[5] S. Lambert, Contribution à l'analyse de l'endommagement par fatigue et au dimensionnement de structures soumises à des vibrations aléatoires, Rouen: thèse à l'INSA de Rouen, 2007.

[6] A. Cristofori, D. Benasciutti and R. Tovo, "A stress invariant based spectral method to estimate fatigue life under multiaxial random loading," *International Journal of Fatigue,* vol. 33, pp. 887-899, 2011.

[7] A. Carpinteri, G. Fortese, C. Ronchei, D. Scorza and A. Spagnoli, "Fatigue life evaluation of metallic structures under multiaxial random loading," *International Journal of Fatigue,* vol. 90, pp. 191-199, 2016.

[8] A. Carpinteri, A. Spagnoli and S. Vantadori, "A review of multiaxial fatigue criteria for random variable amplitude loads," *Fatigue & Fracture of Engineering Materials & Structures,* vol. 40, pp. 1007-1036, 2017.

[9] D. Benasciutti, F. Sherratt and A. Cristofori, "Recent developments in frequency domain multi-axial fatigue analysis," *International Journal of Fatigue,* vol. 91, p. 397–413, 2016.

[10] B. Crossland, "Effect of large hydrostatic pressures on the tortional fatigue strength of an alloy steel," *Proceeding of international conferance on fatigue of metals,* pp. 138-49, 1956.

[11] G. Sines, "Behaviour of metals under complex static and alternationg stress.," *McGraw-Hill,* pp. 145-69, 1959.

[12] P. J. Forsyth, "Fatigue damage and crack growth in aluminium alloys," *Acta Metallurgica,* vol. 11, no. 7, pp. 703-715, 1963.

[13] G. Matsubara and K. Nishio, "Multiaxial high-cycle fatigue criterion considering crack initiation and non-propagation," *International Journal of Fatigue,* vol. 47, p. 222–231, 2013.

[14] G. Matsubra and K. Nishio, "Multiaxial high-cycle fatigue criterion for notches and superficial small holes from considerations of crack initiation and non-propagation," *International Journal of Fatigue,* vol. 67, p. 28–37, 2014.

[15] G. Matsubara, A. Hayashida and D. Kano, "Predicting the multiaxial fatigue limit and the multiaxial high-cycle fatigue life based on the unified equivalent shear stress from axial strength," *International Journal of Fatigue,* vol. 112, p. 52–62, 2018.

[16] A. Yaich, A. El Hami, L. Walha and Haddar M, "Local multiaxial fatigue damage estimation for structures under random vibrations," *Finite Elements in Analysis and Design,* vol. 132, pp. 1-7, 2017.

[17] A. Yaich, G. Kharmanda, A. El Hami, L. Walha and M. Haddar, "Reliability Based Design Optimization for multiaxial fatigue damage analysis using Robust Hybrid Method," *Journal of Mechanics,* vol. 44, pp. 1-16, 2017.

[18] H. Nisitani and N. Yamasita, "Effect of mean stress on initiation and growth of fatigue crack in 70/30 Brass," *Trans JSME,* vol. 32, p. 1456–61, 1966.

[19] H. Nisitani and Y. Hasuo, "Effect of mean stress on tension compression fatigue process of the hardened and tempered S50C," *Trans JSME,* vol. 44, p. 1–7, 1978.

[20] H. Nisitani and M. Goto, "Effect of mean stress on initiation and initial growth of fatigue crack in tension compression fatigue of annealed S45C," *Trans JSME,* vol. 50, p. 1926–35, 1984.

[21] K. Ohji, M. Tsuji, S. Kubo, Y. Ono, A. Yahata and K. Umei, "Predictions of fatigue crack propagation path and life of high-tension steel in residual stress fields," *Trans JSME Ser A,* vol. 59, p. 1429–36, 1993.

[22] B. Li and M. Freitas, "A procedure for fast evaluation of high-cycle fatigue under multiaxial random loading," *Journal of Mechanical design ,* pp. 558-563, 2002.

[23] J. Balthazar and L. Malcher, A review on the main approches for determinationof the multiaxial high cycle fatigue strengh, Brazil: Marcilio Alves & da costa Mattos, 2007.

[24] A. Bernasconi, "Efficient algorithms for calculation of shear stress amplitude and amplitude of the second invariant of the stress deviator in fatigue criteria applications," *International journal of fatigue,* vol. 24, p. 649–657, 2002.

[25] J. Papuga, "Mapping of fatigue damages program shell of FE-calculation. PhD thesis," Faculty of mechanical engineering, Prague, 2005.

[26] A. Cristofori, L. Susmel and A. Tovo, "A stress invariant based criterion to estimate fatigue damage under multiaxial loading," *International Journal of Fatigue,* vol. 30, p. 1646–1658, 2008.

[27] J. Liu and H. Zenner, "Fatigue limit of ductile metals under multiaxial loading," in *Biaxial/Multiaxial Fatigue and Fracture, 6 International Conference on Biaxial/Multiaxial Fatigue and Fracture*, vol. 31, Lisbon, Portugal, Elsevier, 2003, p. 147–164.

[28] C. Gonçalves, J. Araujo and E. Mamiya, "A simple multiaxial fatigue criterion for metals," *Comptes Rendus Mécanique,* vol. 332, pp. 963-968, 2004.

[29] N. Zouain, E. Mamiya and F. Comes, "Using enclosing ellipsoids in multiaxial fatigue strength criteria," *European Journal of Mechanics - A/Solids,* vol. 25, pp. 51-71, 2006.

[30] X. Pitoiset, "Méthodes spectrales pour une analyse en fatigue des structures métallique sous chargements aléatoires multiaxiaux," thèse à l'Université Libre de Bruxelles, Bruxelles, 2001.

[31] A. G. Davenport, "Note on the distribution of largest values of random function with application to gust loading," *Proceedings of the Institution of Civil Engineers,* vol. 28, pp. 187-196, 1964.

[32] D. Benasciutti and A. Cristofori, "A frequency-domain formulation of MCE method for multiaxial random loading," *Fatigue fract. Eng. Master. Struct.,* vol. 31, pp. 937-948, 2008.

[33] S. Lambert, E. Pagnacco and L. Khalij, "A probabilistic model for the fatigue reliability of structures under random loadings with phase shift effects," *International Journal of Fatigue,* pp. 463-474, 2010.

[34] S. LIANG, P.-B. GNING and L. GUILLAUMAT, "A comparative study of fatigue behaviour of flax/epoxy and glass/epoxy composites," *Composites Science and Technology,* vol. 72, no. 5, pp. 535-543, 2012.